ACS OMEGA

Article

Cite This: ACS Omega 2018, 3, 15380−15388

http://pubs.acs.org/journal/acsodf

Enhanced Solubility of Telmisartan Phthalic Acid Cocrystals within the pH Range of a Systemic Absorption Site

Sudeshna Kundu,[†] Nimmy Kumari,[†] Saundray Raj Soni,[†] Subham Ranjan,[§] Rajan Kumar,[‡] Ashoke Sharon,*[,‡] and Animesh Ghosh*[,†]

[†]Department of Pharmaceutical Sciences and Technology and [‡]Department of Chemistry, Birla Institute of Technology, Mesra, Ranchi 835215, India

[§]Department of Chemical Sciences, Indian Institute of Science Education and Research (IISER) Kolkata, Mohanpur Campus, Mohanpur 741252, India

Supporting Information

ABSTRACT: Telmisartan (TLM), a nonpeptide angiotensin II antagonist, is widely prescribed for treating arterial hypertension and marketed by the innovator with the trade name of Micardis and Micardis plus. Telmisartan exhibits low aqueous solubility in the pH range of 3−7, which is the physiological pH. For addressing the issue of poor solubility of TLM, its commercial form makes use of inorganic alkalinizers. The present work illustrates the attempt to improve the solubility of telmisartan via a crystal engineering approach. A novel solid form of telmisartan with phthalic acid was obtained through the solution crystallization method (TPS) and the reaction crystallization method (TPR). Both the forms (TPS and TPR) were thoroughly characterized by powder diffraction X-ray diffraction, differential scanning calorimetry, thermogravimetric analysis, Fourier transform infrared spectroscopy, and ^{1}H NMR and were identified to be two different crystalline forms. Solubility studies of TPS and TPR were conducted at varying pH of phosphate buffer, and they exhibited 11-fold and 22-fold increased solubility, respectively, when compared to that of the pure drug at pH 5, which is within the pH of small intestine at which telmisartan is best absorbed orally from the systemic circulation.

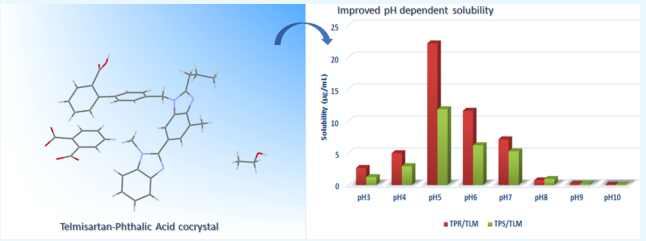

INTRODUCTION

With the rise in the number of poorly soluble drugs in the pipeline and market place, manipulating aqueous solubility of these drugs has become a crucial step in preformulation research. Physicochemical properties of an active pharmaceutical ingredient (API), such as solubility, dissolution, bioavailability, stability, etc., are directed by the arrangement of molecules in its three-dimensional crystal lattice.[1,2] Thus, a variation in the structural arrangement of an API in its solid state through noncovalent interactions will aid in the development of an ideal crystal form with desired properties, and, at the same time, the intrinsic biological activity will be retained. Through exploitation of the crystal engineering technique, it has been possible to anticipate probable intermolecular interactions and design new solid forms with desired properties.[3,4] This in turn has spurred the growth and development of multicomponent solid forms such as salt,[5,6] cocrystals,[7−9] etc. and proved to be a promising approach to address issues such as poor solubility,[10−12] dissolution,[13] bioavailability,[14] stability,[15,16] mechanical properties,[17,18] etc.

In this regard, we aimed to investigate the applicability of the crystal engineering technique and explore a novel solid form of a poorly soluble drug, telmisartan (TLM). Telmisartan (TLM, Figure 1), chemically referred to as 2-[4-[[4-methyl-6-(1-methylbenzimidazol-2-yl)-2-propylbenzimidazol-1-yl]methyl]-phenyl]benzoic acid, is a nonpeptide angiotensin II antagonist,

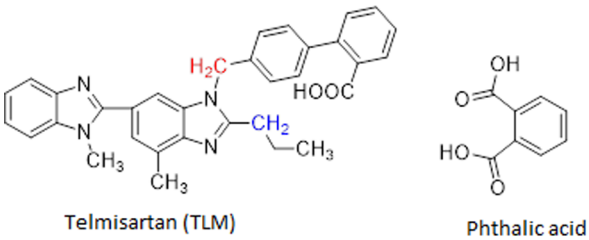

Figure 1. Chemical structure of telmisartan (TLM) highlighting distinguished CH_2 in color and phthalic acid (PA) used in this study.

prescribed for the treatment of arterial hypertension.[19] TLM exists in three crystalline forms, two polymorphs and one pseudopolymorph.[20] The aqueous solubility of TLM is strongly pH-dependent. The maximum solubility was observed at extremely low and high pH. TLM is practically insoluble at pH 3−7 (0.09 μg/mL in water), which is the physiological pH.[19] This poor solubility becomes a major hurdle in the bioavailability of TLM, which is only 42−58%. Nonetheless, TLM is commercially available and marketed by the innovator under the trade name of Micardis and Micardis plus. To

Received: August 23, 2018
Accepted: October 29, 2018
Published: November 13, 2018

DOI: 10.1021/acsomega.8b02144
ACS Omega 2018, 3, 15380−15388

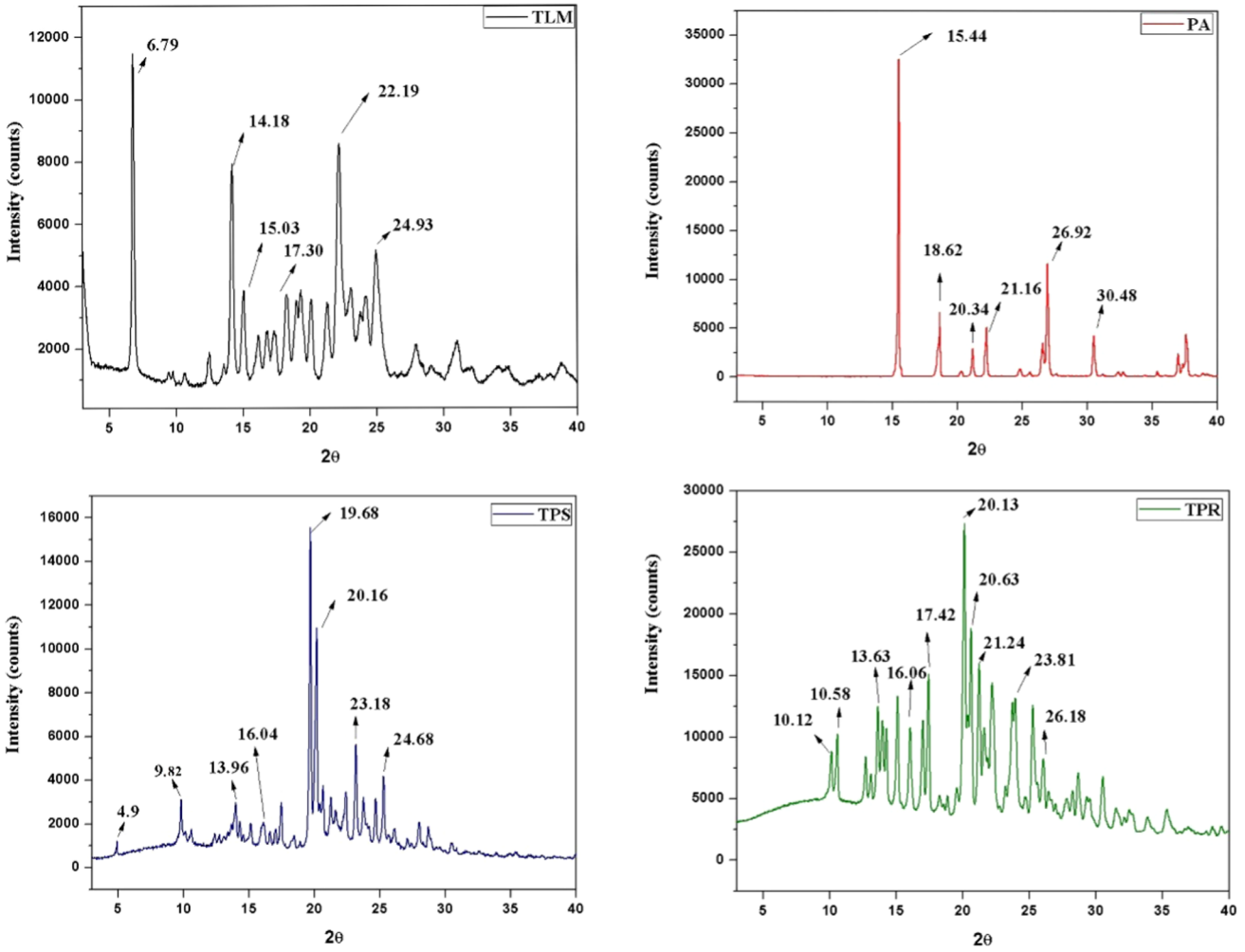

Figure 2. Powder X-ray diffractograms of TPS and TPR compared with those of starting materials.

resolve the issue of pH-dependent solubility of TLM, the marketed formulations make use of strong alkalinizers such as sodium hydroxide, potassium hydroxide, meglumine, or combination thereof as pH modulators.[21] The inorganic alkalinizers increase the microenvironmental pH for achieving the optimum solubility required for absorption. However, this leads to disruption and degeneration of duodenal and jejunal mucosal tissues.[22] Apart from the solubility issues, telmisartan is rapidly absorbed throughout the gastrointestinal tract.[23] However, the maximum absorption is found to be in the small intestine where the intraluminal pH is within the range of 5−7.[23,24] Therefore, the aim of our study is to improve the aqueous solubility of telmisartan within the pH range of small intestine (pH 5−7) to achieve the best possible oral absorption without using any alkalinizers. In comparison with formulation approaches for improving the solubility of telmisartan,[25−28] the investigations through the crystal engineering approach are less and limited to only four reports in the literature.[29−32] Hence, there is a need to limit the use of inorganic alkalinizers and find a suitable crystal form of TLM that can address its poor aqueous solubility and may be an alternative to the existing dosage form.

In this article, we describe the screening studies for a new solid form of telmisartan, isolation and preparation of novel multicomponent solid forms (TPS and TPR) of telmisartan with phthalic acid (PA, Figure 1), and their comprehensive characterization by powder X-ray diffraction (PXRD), ^{1}H NMR, differential scanning calorimetry (DSC), thermogravimetric analysis (TGA), and Fourier transform infrared spectroscopy (FTIR) followed by solubility measurements at various pH.

RESULTS AND DISCUSSION

The structure of TLM possesses one acidic and two basic functionalities, or, in other words, it offers one hydrogen bond donor and two acceptor sites. Thus, it is expected to form hydrogen bonds with certain coformers that are having acid or amide functional groups. For modulating pH-dependent solubility, pK_a of the coformers was also taken into consideration. Therefore, in this study, a series of coformers containing carboxylic group and amide group with varying pK_a values were selected for the screening purpose (Table S1, Supporting Information) by employing the solution crystallization method. A novel multicomponent solid form of telmisartan with phthalic acid was obtained by the solution crystallization method (TPS), which was further prepared by the reaction crystallization method (TPR). The obtained forms (TPS and TPR) were characterized through various analytical techniques.

Powder X-ray Diffraction Analysis. The PXRD pattern with new diffraction peaks and absence of characteristic peaks of the individual components confirms that a new crystalline

DOI: 10.1021/acsomega.8b02144
ACS Omega 2018, 3, 15380−15388

form is produced as the peaks are representatives of reflections of each atomic plane.[33] The characteristic peak of TLM appeared at 2θ values of 6.8, 14.18, 20.10, and 22.19, and phthalic acid showed the characteristic reflection at 15.44, 18.62, and 26.92. The PXRD pattern of TPS and TPR compared with the starting material, telmisartan (TLM) and phthalic acid (PA), is presented in Figure 2. The PXRD pattern revealed that the characteristic peaks of the drug and coformer were absent in it. New diffraction peaks at 2θ values of 4.9, 12.76, 17.04, 22.62, 25.3, 28.02, and 28.72 were observed in TPS. In TPR, unique diffraction peaks were present at 2θ values of 13.12, 13.98, 17.04, 20.66, 23.94, 25.32, 28.32, and 28.72. The characteristic peaks of telmisartan and phthalic acid shifted, and the appearance of new peaks in TPS and TPR confirmed the formation of a new crystalline phase. The literature suggests that various methods used for the synthesis of cocrystals do not lead to the production of the same cocrystal form or composition.[34] Chow et al. suggested that accelerated crystallization by rapid solvent removal often yields a metastable solid, as speculated by Ostwald's rule of successive stages.[34] In this case too, the obtained TPS and TPR possess different cocrystalline forms owing to their different synthesis methods. The difference in the PXRD pattern, thermal behavior, and solubility studies of TPR and TPS proved the same.

Calculation of Stoichiometric Proportion in TPS and TPR. Solution ^{1}H NMR was used to identify and confirm the chemical components and the stoichiometry in the new crystalline phase.[35,36] The resulting ^{1}H NMR spectrum of the TPS and TPR cocrystal systems comprises the peaks from TLM, PA, and ethanol. It is evident from NMR that the acidic protons from the carboxylic group of TPS and TPR are in downfield at 13.35 ppm (Figure S1) and 13.26 ppm (Figure S4), respectively, which confirms H-bonded acidic protons and voids any proton transfer. This study further confirms the existence of a solvated cocrystal for both TPS and TPR. Both the D_2O exchange spectra of TPS (Figure S1) and TPR (Figure S5) show the disappearance of the peaks corresponding to acidic protons. The peak assignment from ^{1}H NMR data confirms the distinguished peak of two CH_2, as shown in blue and red (Figure 1) at δ 2.90 (t, 2H) and δ 5.54 (s, 2H), respectively, for TLM in the TPS cocrystal system. A total of 14 aromatic protons (ArHs) appear as multiples in the region of δ 7.14−7.57. Furthermore, phthalic acid has 4 ArHs as multiplets in the region of δ 7.64−7.69, which merge with aromatic protons of TLM. The relative integration of distinguished CH_2 (red as in Figure 1) of TLM at δ 5.54 shows integration of 2H and 18H found in the aromatic region. Thus, quantitative integration (Figure S2) confirms the 1:1 ratio of TLM (14 ArHs) and PA (4 ArHs) in the TPS cocrystal system. Similar results were obtained for the TPR cocrystal system, which confirmed the 1:1 ratio of TLM (14 ArHs) and PA (4 ArHs) in this system. In another quantitative integration study from ^{1}H NMR spectrum of TPS cocrystal system showing distinguished CH_2 peak of TLM (blue δ: 2.90, t, 2H) with 1 integration in comparison to 0.5 integration for CH_2 proton of ethanol (δ: 3.35−3.40). Thus, the presence of half ratio of ethanol in comparison to unit ratio of TLM confirms the presence of TLM/ethanol in 1:0.5 ratio (Figure S3) in TPS cocrystal. Thus, overall, the ratio of TLM, PA, and ethanol was stoichiometrically confirmed as 1:1:0.5 in the TPS cocrystal system. Similar quantitative integration studies were conducted to identify the stoichiometric proportion of TLM, PA, and ethanol in the TPR cocrystal system, and it was found to be 1:1:0.3, as shown in Figure S5.

It is interesting to note that the presence of TLM, PA, and ethanol was further confirmed through single-crystal X-ray diffraction (SCXRD) analysis. The asymmetric unit comprises TLM, PA, and ethanol in the TPS cocrystal, as shown in the Oak Ridge Thermal Ellipsoid Plot (ORTEP) diagram with 30% probability displacement ellipsoids (Figure 3).[37] The single-crystal parameters of TPS are mentioned in the foot note of Figure 3.

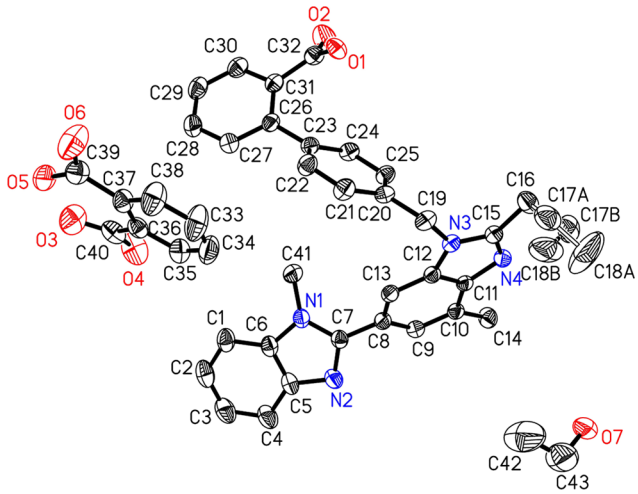

Figure 3. X-ray crystal structure of the TPS cocrystal showing the ORTEP diagram using a 30% ellipsoidal plot. Telmisartan (TLM), phthalic acid (PA), and ethanol were found in the asymmetric unit, and hydrogen atoms are not shown for clarity. $C_{43}H_{42}N_4O_7$, M = 726.81, monoclinic, space group: I 2/a, a = 15.9027(10), b = 13.2297(9), c = 36.609(2) Å, α = 90.000(0), β = 99.754(6), γ = 90.000(0), V = 7590.7(8) Å^3, T = 293(2) K, Z = 8, μ = 0.087 mm^{-1}, F(000) = 3072.0, Dc = 1.272 Mg/m, crystal size: 0.15 × 0.12 × 0.10 mm, 140 72 reflections measured, 6687 unique, R1 = 0.0741 for 4357 Fo > 4σ(Fo) and 0.1075 for all 6687 data and 528 parameters. Unit cell determination and intensity data collection were performed with 99% completeness at 293(2) K. Structure solutions by direct methods and refinements by full-matrix least-squares methods on F2 [CCDC No: 1520132].

Thermal Analysis. The distinct melting points of TPS and TPR from those of TLM (270.24 °C) and PA (209.94 °C) suggested the formation of a new crystalline phase. However, TPS and TPR exhibited an unfamiliar thermal behavior (Figures 4A and 5A). Desolvation of the ethanol molecule occurred in TPS and TPR at 124 and 156 °C, respectively, indicating the different binding energy of ethanol in TPS and TPR. Melting of desolvated TPS and TPR was observed at 199.8 °C, heat of fusion (ΔH_f) = 136.40 J/g, and at 200.53 °C, ΔH_f = 157.66 J/g, respectively. Upon desolvation, TPS and TPR converted into the same form, similar to the phenomenon observed in the telmisartan−saccharine cocrystal.[29] The melting of desolvated TPS and TPR was found to be accompanied by decomposition of PA (endothermic event) and subsequent recrystallization (exothermic event) of TLM. The recrystallization peak of TLM does not appear in any of the DSC thermogram due to partial cancellation of the exothermic and endothermic events occurring simultaneously.[38,39] Surprisingly, the endothermic melting peak of recrystallized TLM did not appear in TPR. A DSC experiment

DOI: 10.1021/acsomega.8b02144
ACS Omega 2018, 3, 15380−15388

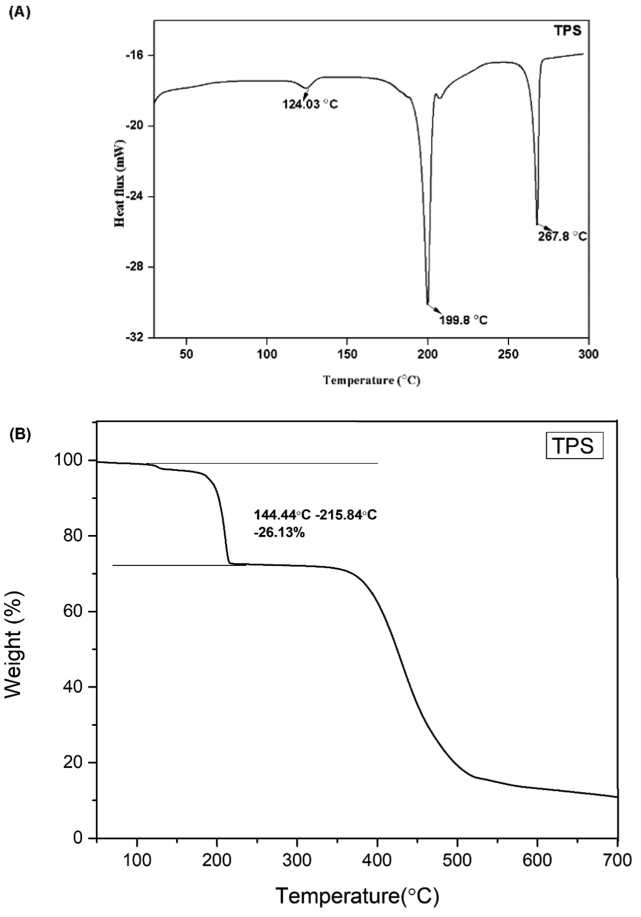

Figure 4. (A) DSC thermogram of TPS and (B) TGA curve of TPS.

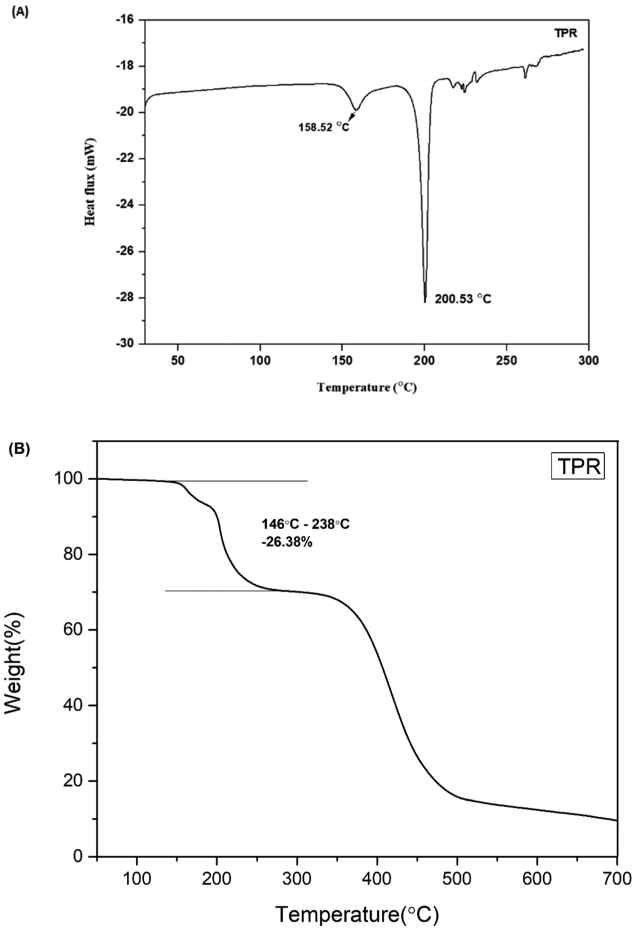

Figure 5. (A) DSC thermogram of TPR and (B) TGA curve of TPR.

was conducted to unveil the reason behind the phenomenon. After melting of the desolvated TPR form, it was isothermally held at 200 °C for 1 h and then cooled to 30 °C to ensure complete recrystallization of TLM from the melt. The endothermic peak of recrystallized TLM appeared in the second heating cycle and is presented in Figure 6.

On analyzing the TGA profile of TPS and TPR (Figures 4B and 5B), there was a weight loss of 26.13 and 26.38% in the temperature range of 144.44−215.84 and 146−238 °C, respectively. The weight loss in TPS corroborates with the theoretical weight loss of 27.16% for the loss of 0.5 mol of ethanol and 1 mol of phthalic acid from the crystal lattice. In the same manner, the weight loss in TPR corroborates with the theoretical weight loss of 25.90% for the loss of 0.3 mol of ethanol and 1 mol of phthalic acid from the crystal lattice. This suggests that stoichiometry of TLM/PA/EtOH in TPS and TPR is 1:1:0.5 and 1:1:0.3, respectively, and this also corroborates with the stoichiometry established from ^{1}H NMR analysis.

Fourier Transform Infrared (FTIR) Spectroscopy. Fourier transform infrared (FTIR) spectroscopy can be used as a reliable technique to detect the formation of the multicomponent crystal. The FTIR spectra of telmisartan, phthalic acid, TPS, and TPR are shown in Figure 7, and relevant bands are presented in Table 1. Carboxylic acid (COOH) absorbs strongly at 1700 cm^{-1} for the C═O stretching band and a weaker C−O stretch around 1200 cm^{-1}, whereas the carboxylate group (COO−) exhibits two characteristic coupled carbonyl absorption band at 1550−

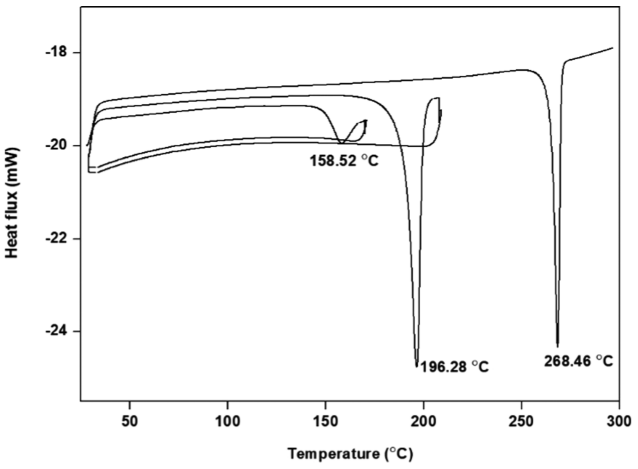

Figure 6. DSC thermogram of TPR (heating−cooling cycle).

1650 cm^{-1} (asymmetric) and around 1400 cm^{-1} (symmetric).[6,12,39,40] The carbonyl stretches of carboxylic acid of TLM were observed at 1697 cm^{-1}, which is not affected and appeared at 1693 cm^{-1} in TPS and TPR. Furthermore, one of the C═O stretches of PA was also merged within 1693 cm^{-1}. The second C═O stretch of PA appeared at 1585 cm^{-1}, which downshifted to 1573 and 1566 cm^{-1} in TPS and TPR, respectively, due to the formation of H-bonding in the cocrystal system. The identification of C−N stretching is rather difficult because the mixing of bands is possible in this region.

DOI: 10.1021/acsomega.8b02144
ACS Omega 2018, 3, 15380−15388

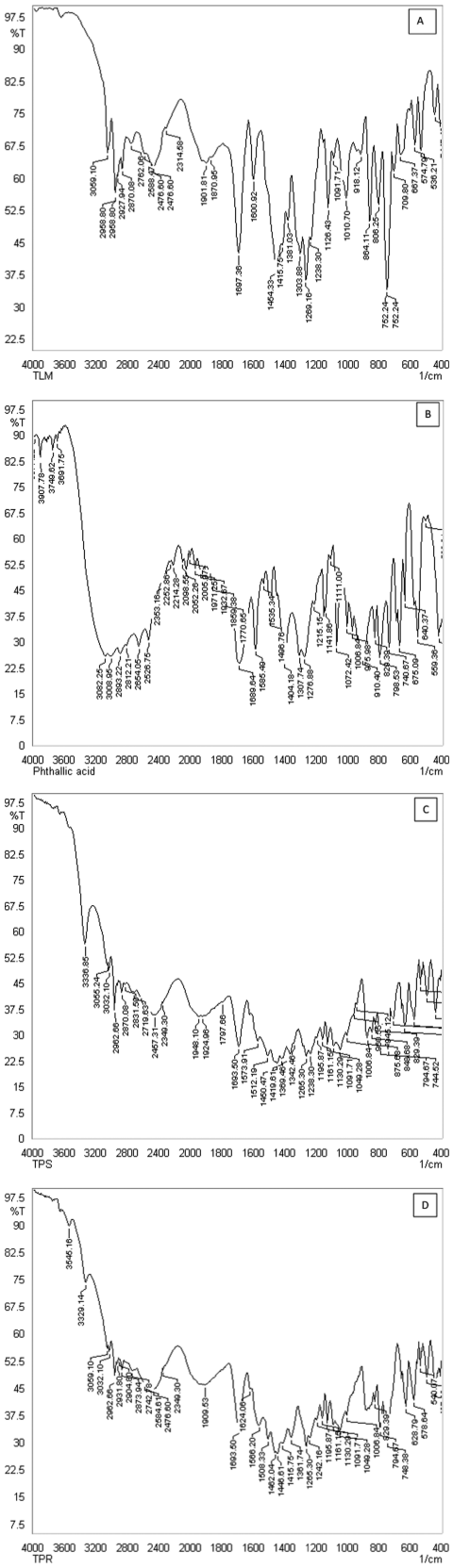

Figure 7. FTIR spectra obtained for (A) TLM (B) PA (C) TPS, (D) TPR.

Hence, the FTIR bands at 1303 and 1381 cm^{-1} have been attributed to the C−N stretching in TLM, which is observed at 1369 and 1361 cm^{-1} for TPS and TPR, respectively.

The appearance of an additional OH stretching vibration at 3032 cm^{-1} in TPS and TPR implies the presence of ethanol in the crystal lattice. The ethanol molecule possibly interacts only with C═O of PA, as there in no change in the C═O stretch of TLM. Thus, the FTIR spectra corroborate with ^{1}H NMR and SCXRD, confirming that the new solid form (TPS, TPR) is a solvated cocrystal.

pH-Dependent Solubility Studies. The pH-dependent solubility of telmisartan is attributed to its three pK_a values 3.5, 4.1, and 6.0 corresponding to its carboxylic (acidic) and two benzimidazole (basic) functional groups, respectively.[19,41,42] At acidic pH, the N of benzimidazole of TLM gets ionized, forming a cationic center, and at basic pH, the carboxylic group of TLM is ionized, forming an anionic center, which is responsible for its maximum solubility at extremely high and low pH. Even though TLM exhibits a good solubility profile at extremely high and low pH, it exhibits low solubility in the pH range of 3−7, i.e., in the physiological pH range. When the cocrystal gets dissolved in aqueous solvent, both the drug and coformer ionize in aqueous solvent; therefore, the solution pH is an important factor in determining its solubility as well as stability. It is important to determine the thermodynamic stability with respect to pH for understanding the transformation of the multicomponent form of telmisartan to its free form. This result will help us achieve the desired dissolution rate and bioavailability over a wide pH range. Thus, the solubility measurement of TPS and TPR was carried out at various pH values in phosphate buffer.

In Figure 8, solubility−pH profiles of telmisartan, TPS, and TPR have been presented. A "U"-shaped solubility−pH profile was obtained for telmisartan due to its amphoteric nature. The ionizing nature of the coformer imparted modification in the solubility−pH profile of telmisartan and increased its solubility at a lower pH. The solubilities of TPS and TPR have been greatly enhanced by 11-fold and 22-fold at solution pH 5, thereby showing its pH dependency, which can be visualized in Figure 9. The systemic absorption of TLM is found to be highest in small intestine where the pH lies in the range of 5−7.[23,43] Thereby, enhanced solubility of telmisartan at its best site of systemic absorption has been achieved through its cocrystalline form.

Due to the acidic nature of the coformer, the solution pH was found to be decreased. Therefore, the equilibrium pH was noted upon completion of the solubility experiment and is presented in Table S2, Supporting Information.

Determination of pH_{max}. Another important aspect in the solubility−pH profile of an ionizable drug (acidic/basic/amphoteric) is the determination of pH_{max}. pH_{max} aids in understanding the stability of the new solid form with respect to pH and subsequently its in vivo and in vitro performance.[44] pH_{max} is referred to as the intersection point of two independent curves, where one curve represents the drug as the saturating or equilibrium species and the other curve represents the salt as the equilibrium species.[45] The same concept holds for determining the pH_{max} of the cocrystal. From Figure 8, pH_{max} of TPS and TPR can be observed at just below pH 8.

Theoretically, when pH is below pH_{max}, the cocrystal is the saturation species; above that, the saturation species is the free base/drug; and pH_{max} is the pH where both the phases coexist. For analyzing this, the residual solids collected from the solubility study of TPS and TPR at different pH were characterized by PXRD and is shown in Figures 10 and 11.

DOI: 10.1021/acsomega.8b02144
ACS Omega 2018, 3, 15380−15388

Table 1. Relevant Bands of TLM, PA, TPS, and TPR in Their FTIR Spectra

	TLM	PA	TPS	TPR
C−O stretching vibrations	1269	1276	1265, 1238	1265, 1242
C−N stretching vibrations	1303, 1381		1369	1361
C═O stretching vibrations	1697	1689, 1585	1693, 1573	1693, 1566
O−H stretching vibrations	3059	3691, 3008	3336, 3055, 3032	3329, 3059, 3032

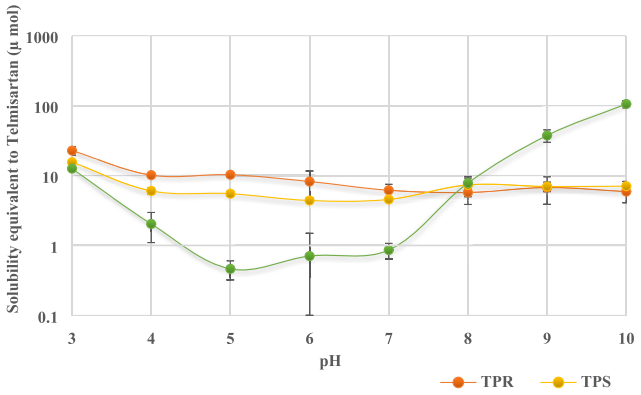

Figure 8. Solubility of TPS, TPR, and TLM at varying pHs (3−10).

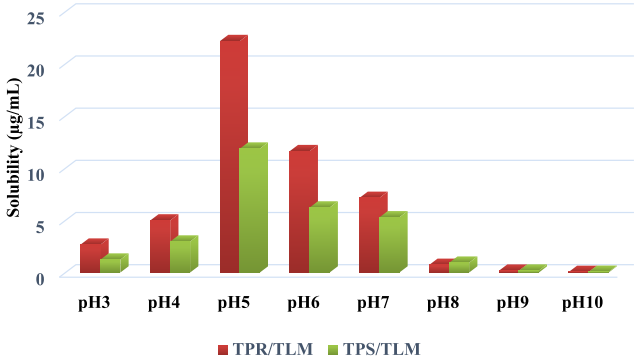

Figure 9. Solubility comparison of TPS, TPR, and TLM at varying pHs (3−10).

The diffraction peaks corresponding to the TPS cocrystal, i.e., at 9.82, 13.96, 19.6, and 20.16, were almost retained in all residual samples collected from the solubility study within the pH of 3−7. Moreover, the diffraction peaks corresponding to the TPR cocrystal at 2θ, 13.63, 17.01, and 20.63, were almost retained in all residual samples collected from the solubility study within the pH of 3−7. In between pHs 6 and 7, for TPS and TPR, both cocrystals and telmisartan were found to be present in the residual solid, confirmed by the appearance of characteristic peaks of telmisartan at 2θ 6.78 and 14.18° in the PXRD diffractogram along with the peaks of TPS and TPR. This may be concluded that the pH_{max} for TPS and TPR lies around pH 7. When pH is above the pH_{max}, the saturated species would be free base, telmisartan. The appearance of characteristic peaks of telmisartan and disappearance of the characteristic peak of TPS and TPR from the PXRD diffractogram from pH 8 (which is above pH_{max}) onwards confirmed that the saturation species is telmisartan. Therefore, the PXRD result corroborated well with the concept of pH_{max} in the case of the cocrystal of basic drugs.

CONCLUSIONS

In conclusion, this work demonstrates the finding of a novel solid form of telmisartan through the crystal engineering approach. Of several coformers used for screening, phthalic acid formed a new multicomponent solid phase with telmisartan. The new multicomponent solid forms were prepared by two methods, namely, the solution crystallization method (TPS) and reaction crystallization method (TPR). Both the forms were characterized by powder X-ray diffraction (PXRD), ^{1}H NMR, differential scanning calorimetry (DSC), thermogravimetric analyses (TGA), and Fourier Transform Infrared Spectroscopy (FTIR). TPS and TPR were found to be

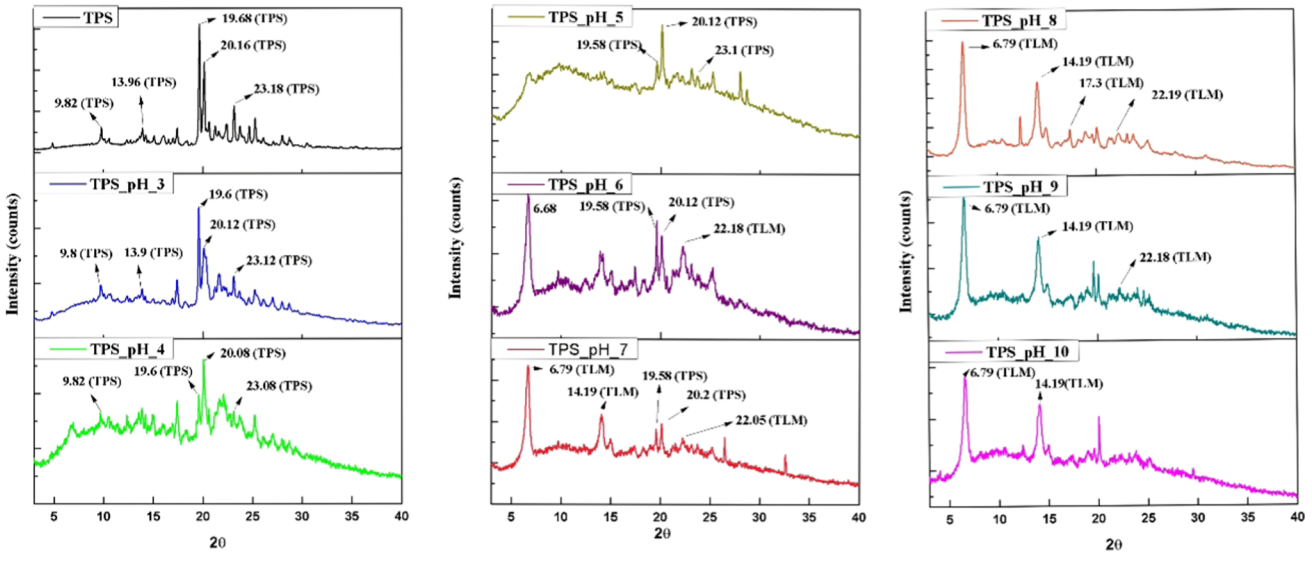

Figure 10. PXRD of residual solids collected from the solubility study of TPS at pH range 3−10.

DOI: 10.1021/acsomega.8b02144
ACS Omega 2018, 3, 15380−15388

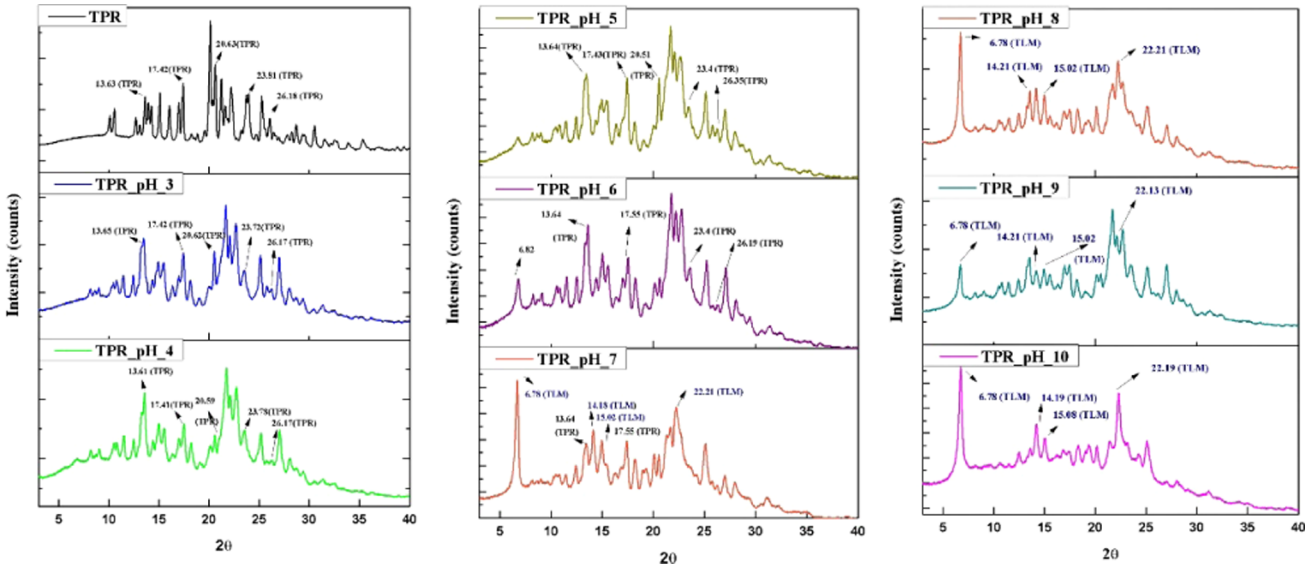

Figure 11. PXRD of residual solids collected from the solubility study of TPR at pH range 3−10.

a solvated cocrystal of telmisartan. The objective of this work of enhancing the solubility of telmisartan within the physiological range was achieved. TPS and TPR markedly increased the solubility of telmisartan by 11-fold and 22-fold at pH 5, the pH at which telmisartan gets absorbed from systemic circulation. The experimental solubility result suggests the selection of coformer to be a crucial step and its pK_a to modulate the physicochemical properties of an amphoteric API. Thus, by the cocrystallization technique it is possible to improve the pH-dependent solubility of telmisartan, which may eliminate the use of inorganic alkalinizers in its marketed dosage form.

EXPERIMENTAL SECTION

Materials. Polymorph A of telmisartan (TLM, 99.7% pure) was obtained as a gift sample from Unichem Laboratories Ltd. (Himachal Pradesh, India). Phthalic acid was procured from Sigma-Aldrich Chemicals and was used without any further purification. The solvents (chloroform, ethanol) used for crystallization were of high-performance liquid chromatography (HPLC) grade (Rankem, India).

Synthesis of the New Solid Form by the Solution Crystallization Method (TPS). Equimolar quantity of telmisartan (25 mg, 0.0485 mmol) and phthalic acid (8.05 mg, 0.0485 mmol) was ground in a mortar and pestle for 10 min and the ground mixture was dissolved in 6−7 mL of chloroform:ethanol (2:1 v/v) and allowed to evaporate at room temperature. After 6−7 days, single crystals of suitable size for XRD analysis were obtained. The formation of a new solid phase was preliminarily confirmed by PXRD and then analyzed by DSC, TGA, FTIR, ^{1}H NMR, and SCXRD.

Synthesis of the New Solid form by the Reaction Crystallization Method (TPR). A saturated solution of telmisartan was prepared in chloroform and ethanol (1:1 v/v). To it, phthalic acid was added in an amount under its solubility limit. The solid precipitate was collected and initially confirmed by PXRD. It was then further analyzed by DSC, TGA, FTIR, and ^{1}H NMR.

Characterization of the New Solid Form. *Powder X-ray Diffraction (PXRD).* PXRD patterns were collected on a Rigaku Smart Lab diffractometer system with a 1.5406 Å radiation wavelength. The tube voltage and current were set at 45 kV and 200 mA, respectively. Each sample was placed in an aluminum sample holder and measured by a continuous scan between 3 and 40° in 2θ with a step size of 0.02°/min at room temperature and with a scan speed of 5°/min using a semiconductor detector. The experimental PXRD patterns were refined using Smart Lab Guidance software.

^{1}H NMR Spectroscopy. ^{1}H NMR analysis of TPS and TPR was performed on a 400 MHz JEOL NMR spectrometer using DMSO-d_6 as a solvent at 25 °C. The D_2O exchange experiment was conducted to identify the chemical shift of acidic protons. Stoichiometry of TPS and TPR cocrystal systems was estimated using relative integration of the distinguished $-CH_2$ peak (Figure 1) of TLM in comparison to distinguished protons of phthalic acid and ethanol.

Single-Crystal X-ray Diffraction Analysis of TPS. X-ray diffraction data were recorded on a SuperNova Eos diffractometer using monochromatic Mo Kα radiation (λ = 0.71073 Å). Data collection was performed at room temperature (293 K) for the samples studied. Olex2 was used to solve the structure using ShelXS and refined with the ShelXL refinement package using least-squares minimization. The observed disordered atoms C17 (C17A and C17B) and C18 (C18A and C18B) from the propyl side chain of TLM were refined using Olex2 and are shown in the ORTEP diagram (Figure 3). All of the nonhydrogen atoms were refined anisotropically, and the hydrogen atoms were placed on the basis of the mixed mode through Fourier difference maps and geometrical assignment.

Differential Scanning Calorimetry (DSC). DSC of all samples was conducted using a DSC 4000 instrument (PerkinElmer). Samples (3−5 mg) were crimped in non-hermetic aluminum pans and scanned from 30 to 300 °C at a heating rate of 5 °C/min under a continuously purged dry nitrogen atmosphere at a constant flow rate (20 mL/min). The data were processed using Pyris manager software.

Thermogravimetric Analysis (TGA). TGA was performed on a TGA 4000 (PerkinElmer) instrument. The samples (5−8 mg) were placed into a ceramic pan and heated from 30 to 700 °C at a rate of 10 °C/min under nitrogen purge at a flow rate

DOI: 10.1021/acsomega.8b02144
ACS Omega 2018, 3, 15380−15388

of 20 mL/min. The data were managed by Pyris manager software.

Fourier Transform Infrared Spectroscopy (FTIR). The infrared spectra of the drug, coformer, and salts were recorded individually by a FTIR-8400S spectrophotometer (Shimadzu, Japan) using the potassium bromide (KBr) pellet method. The IR absorption spectra of samples with 50 scans were measured over the range of 4000−500 cm^{-1} with a resolution of 4 cm^{-1} for each sample. The data were analyzed using IR solution software.

Solubility Measurement. All solubility measurements were carried out in phosphate buffer at 25 °C. pH was adjusted with potassium hydroxide and hydrochloric acid. Aliquots (0.2 mL) were withdrawn at 72 and 96 h (for ensuring equilibrium conditions) and filtered through a 0.45 μm syringe filter (AXIVA). The concentrations of telmisartan and phthalic acid were analyzed by an HPLC system (Waters TM 486, tunable absorbance detector) equipped with a UV/Vis detector. A C18 Nova-Pak column (5 μm, 4.6 × 250 mm) at ambient temperature with a flow rate of 1 mL/min was used to separate telmisartan and phthalic acid. An isocratic method with methanol and phosphate buffer (10 mM) mixed in a ratio of 72:28 (v/v) was opted for quantitative determination of telmisartan and phthalic acid at an optimum wavelength of 296 nm. Sample injection was 20 μL. EMPOWER software was used for collection and processing the data. The concentrations of telmisartan and phthalic acid were calculated using the standard curve (linearity range 2−16 μg/mL for both the analytes), which was prepared in a mobile phase. The samples were diluted by methanol prior to analysis. The experiments were conducted in triplicate and were expressed as mean ± standard deviation.

■ ASSOCIATED CONTENT

Supporting Information

The Supporting Information is available free of charge on the ACS Publications website at DOI: 10.1021/acsomega.8b02144.

Screening list information; ^{1}H NMR spectra; and equilibrium solution pH of TLM, TPS, and TPR (PDF)

■ AUTHOR INFORMATION

Corresponding Authors

*E-mail: aghosh@bitmesra.ac.in, anim_1607@yahoo.co.in. Phone: +91-651-2276247. Fax: +91-651-2275290 (A.G.).
*E-mail: asharon@bitmesra.ac.in. Phone: +91-651-2276531. Fax: +91-651-2275401 (A.S.).

ORCID

Ashoke Sharon: 0000-0001-5738-1607
Animesh Ghosh: 0000-0002-2990-4738

Notes

The authors declare no competing financial interest.

■ ACKNOWLEDGMENTS

A.G. acknowledges financial support from SERB, DST (EMR/2014/000099). A.G. sincerely acknowledges support of ACS in form of ACS Author Reward (ARRESJESMK40K9ZJ8AN7) which has been redeemed to purchase an open access license (Author Choice) for this article. S.R. thanks the INSPIRE fellowship from the Department of Science and Technology, Govt. of India. The authors acknowledge X-ray diffraction data collection from IISER Kolkata. The authors are also thankful to BIT Mesra, Ranchi, for NMR facility (DST FIST: SR/FST/CSI-242/2012) and Central Instrumentation Facility for analytical & characterization studies.

■ REFERENCES

(1) Qiao, N.; Li, M.; Schlindwein, W.; Malek, N.; Davies, A.; Trappitt, G. Pharmaceutical cocrystals: an overview. *Int. J. Pharm.* **2011**, *419*, 1−11.
(2) Schultheiss, N.; Newman, A. Pharmaceutical cocrystals and their physicochemical properties. *Cryst. Growth Des.* **2009**, *9*, 2950−2967.
(3) Desiraju, G. R. Crystal engineering: from molecule to crystal. *J. Am. Chem. Soc.* **2013**, *135*, 9952−9967.
(4) Aakeröy, C. B.; Champness, N. R.; Janiak, C. Recent advances in crystal engineering. *CrystEngComm* **2010**, *12*, 22−43.
(5) Mannava, M. K. C.; Suresh, K.; Nangia, A. Enhanced bioavailability in the oxalate salt of the anti-tuberculosis drug ethionamide. *Cryst. Growth Des.* **2016**, *16*, 1591−1598.
(6) Maddileti, D.; Swapna, B.; Nangia, A. High solubility crystalline pharmaceutical forms of blonanserin. *Cryst. Growth Des.* **2014**, *14*, 2557−2570.
(7) Bhandaru, J. S.; Malothu, N.; Akkinepally, R. R. Characterization and solubility studies of pharmaceutical cocrystals of eprosartan mesylate. *Cryst. Growth Des.* **2015**, *15*, 1173−1179.
(8) Sugandha, K.; Kaity, S.; Mukherjee, S.; Isaac, J.; Ghosh, A. Solubility enhancement of ezetimibe by a cocrystal engineering technique. *Cryst. Growth Des.* **2014**, *14*, 4475−4486.
(9) Ranjan, S.; Devarapalli, R.; Kundu, S.; Vangala, V. R.; Ghosh, A.; Reddy, C. M. Three new hydrochlorothiazide cocrystals: Structural analyses and solubility studies. *J. Mol. Struct.* **2017**, *1133*, 405−410.
(10) Chadha, R.; Saini, A.; Khullar, S.; Jain, D. S.; Mandal, S. K.; Guru Row, T. Crystal structures and physicochemical properties of four new lamotrigine multicomponent forms. *Cryst. Growth Des.* **2013**, *13*, 858−870.
(11) Goud, N. R.; Suresh, K.; Nangia, A. Solubility and stability advantage of aceclofenac salts. *Cryst. Growth Des.* **2013**, *13*, 1590−1601.
(12) Mittapalli, S.; Mannava, M. C.; Khandavilli, U. R.; Allu, S.; Nangia, A. Soluble salts and cocrystals of clotrimazole. *Cryst. Growth Des.* **2015**, *15*, 2493−2504.
(13) Shiraki, K.; Takata, N.; Takano, R.; Hayashi, Y.; Terada, K. Dissolution improvement and the mechanism of the improvement from cocrystallization of poorly water-soluble compounds. *Pharm. Res.* **2008**, *25*, 2581−2592.
(14) McNamara, D. P.; Childs, S. L.; Giordano, J.; Iarriccio, A.; Cassidy, J.; Shet, M. S.; Mannion, R.; O'donnell, E.; Park, A. Use of a glutaric acid cocrystal to improve oral bioavailability of a low solubility API. *Pharm. Res.* **2006**, *23*, 1888−1897.
(15) Tsutsumi, S.; Iida, M.; Tada, N.; Kojima, T.; Ikeda, Y.; Moriwaki, T.; Higashi, K.; Moribe, K.; Yamamoto, K. Characterization and evaluation of miconazole salts and cocrystals for improved physicochemical properties. *Int. J. Pharm.* **2011**, *421*, 230−236.
(16) Trask, A. V.; Motherwell, W. S.; Jones, W. Physical stability enhancement of theophylline via cocrystallization. *Int. J. Pharm.* **2006**, *320*, 114−123.
(17) Krishna, G. R.; Shi, L.; Bag, P. P.; Sun, C. C.; Reddy, C. M. Correlation among crystal structure, mechanical behavior, and tabletability in the co-crystals of vanillin isomers. *Cryst. Growth Des.* **2015**, *15*, 1827−1832.
(18) Bag, P. P.; Chen, M.; Sun, C. C.; Reddy, C. M. Direct correlation among crystal structure, mechanical behaviour and tabletability in a trimorphic molecular compound. *CrystEngComm* **2012**, *14*, 3865−3867.
(19) Wienen, W.; Entzeroth, M.; Meel, J. C.; Stangier, J.; Busch, U.; Ebner, T.; Schmid, J.; Lehmann, H.; Matzek, K.; Kempthorne-Rawson, J.; et al. A review on telmisartan: A novel, long-acting

DOI: 10.1021/acsomega.8b02144
ACS Omega 2018, 3, 15380−15388

angiotensin II-receptor antagonist. *Cardiovasc. Drug Rev.* **2000**, *18*, 127−154.
(20) Dinnebier, R. E.; Sieger, P.; Nar, H.; Shankland, K.; David, W. I. Structural characterization of three crystalline modifications of telmisartan by single crystal and high-resolution X-ray powder diffraction. *J. Pharm. Sci.* **2000**, *89*, 1465−1479.
(21) Park, J.; Park, H. J.; Cho, W.; Cha, K.-H.; Yeon, W.; Kim, M.-S.; Kim, J.-S.; Hwang, S.-J. Comparative study of telmisartan tablets prepared via the wet granulation method and pritor prepared using the spray-drying method. *Arch. Pharm. Res.* **2011**, *34*, No. 463.
(22) Phuong, H.-L. T.; Tran, T. T.-D.; Lee, S. A.; Nho, V. H.; Chi, S.-C.; Lee, B.-J. Roles of MgO release from polyethylene glycol 6000-based solid dispersions on microenvironmental pH, enhanced dissolution and reduced gastrointestinal damage of telmisartan. *Arch. Pharm. Res.* **2011**, *34*, No. 747.
(23) Shimasaki, M.; Yamashita, K.; Imanishi, R.; Yokoyama, K.; Kuritani, M.; Oiwa, Y.; Igarashi, T. Pharmacokinetics of 14C-telmisartan (1): absorption, distribution and protein binding of 14C-telmisartan after a single oral administration to rats. *Drug Metab. Pharmacokinet.* **1999**, *14*, 425−431.
(24) Schmaljohann, D. Thermo-and pH-responsive polymers in drug delivery. *Adv. Drug Delivery Rev.* **2006**, *58*, 1655−1670.
(25) Borba, P. A. A.; Pinotti, M.; Andrade, G. R. S.; da Costa, N. B., Jr.; Junior, L. R. O.; Fernandes, D.; de Campos, C. E. M.; Stulzer, H. K. The effect of mechanical grinding on the formation, crystalline changes and dissolution behaviour of the inclusion complex of telmisartan and *β*-cyclodextrins. *Carbohydr. Polym.* **2015**, *133*, 373−383.
(26) Lepek, P.; Sawicki, W.; Wlodarski, K.; Wojnarowska, Z.; Paluch, M.; Guzik, L. Effect of amorphization method on telmisartan solubility and the tableting process. *Eur. J. Pharm. Biopharm.* **2013**, *83*, 114−121.
(27) Zhang, Y.; Zhi, Z.; Jiang, T.; Zhang, J.; Wang, Z.; Wang, S. Spherical mesoporous silica nanoparticles for loading and release of the poorly water-soluble drug telmisartan. *J. Controlled Release* **2010**, *145*, 257−263.
(28) Isaac, J.; Ganguly, S.; Ghosh, A. Co-milling of telmisartan with poly (vinyl alcohol)—An alkalinizer free green approach to ensure its bioavailability. *Eur. J. Pharm. Biopharm.* **2016**, *101*, 43−52.
(29) Chadha, R.; Bhandari, S.; Haneef, J.; Khullar, S.; Mandal, S. Cocrystals of telmisartan: characterization, structure elucidation, in vivo and toxicity studies. *CrystEngComm* **2014**, *16*, 8375−8389.
(30) Alatas, F.; Ratih, H.; Soewandhi, S. N. Enhancement of solubility and dissolution rate of telmisartan by telmisartan-oxalic acid cocrystal formation. *Int. J. Pharm. Pharm. Sci.* **2015**, *7*, 423−426.
(31) Donsbach, K.; Hof, I. Crystalline Form of Telmisartan Sodium. U.S. Patent US6737432B22006.
(32) Arora, P.; Kaur, A.; Haneef, J.; Chadha, R. Solubility improvement of telmisartan by cocrystallization with citric acid. *Int. J. Pharm. Sci. Res.* **2017**, *8*, 3768−3775, DOI: 10.13040/IJPSR.0975-8232.8(9).3962-65.
(33) Fultz, B.; Howe, J. Diffraction and the X-ray Powder Diffractometer. In *Transmission Electron Microscopy and Diffractometry of Materials*; Springer, 2013; pp 1−57.
(34) Chow, S. F.; Shi, L.; Ng, W. W.; Leung, K. H. Y.; Nagapudi, K.; Sun, C. C.; Chow, A. H. Kinetic entrapment of a hidden curcumin cocrystal with phloroglucinol. *Cryst. Growth Des.* **2014**, *14*, 5079−5089.
(35) Deng, J.-H.; Lu, T.-B.; Sun, C. C.; Chen, J.-M. Dapagliflozin-citric acid cocrystal showing better solid state properties than dapagliflozin. *Eur. J. Pharm. Sci.* **2017**, *104*, 255−261.
(36) Shimpi, M. R.; Childs, S. L.; Boström, D.; Velaga, S. P. New cocrystals of ezetimibe with L-proline and imidazole. *CrystEngComm* **2014**, *16*, 8984−8993.
(37) Dolomanov, O. V.; Bourhis, L. J.; Gildea, R. J.; Howard, J. A. K.; Puschmann, H. OLEX2: a complete structure solution, refinement and analysis program. *J. Appl. Crystallogr.* **2009**, *42*, 339−341.
(38) Caira, M. R.; Bourne, S. A.; Samsodien, H.; Engel, E.; Liebenberg, W.; Stieger, N.; Aucamp, M. Co-crystals of the antiretroviral nevirapine: crystal structures, thermal analysis and dissolution behaviour. *CrystEngComm* **2012**, *14*, 2541−2551.
(39) Chadha, R.; Singh, P.; Khullar, S.; Mandal, S. K. Ciprofloxacin Hippurate Salt: Crystallization Tactics, Structural Aspects, and Biopharmaceutical Performance. *Cryst. Growth Des.* **2016**, *16*, 4960−4967.
(40) Adalder, T. K.; Sankolli, R.; Dastidar, P. Homo-or heterosynthon? A crystallographic study on a series of new cocrystals derived from pyrazinecarboxamide and various carboxylic acids equipped with additional hydrogen bonding sites. *Cryst. Growth Des.* **2012**, *12*, 2533−2542.
(41) Cagigal, E.; Gonzalez, L.; Alonso, R.; Jimenez, R. pK_a determination of angiotensin II receptor antagonists (ARA II) by spectrofluorimetry. *J. Pharm. Biomed. Anal.* **2001**, *26*, 477−486.
(42) Dukeck, R.; Sieger, P.; Karmwar, P. Investigation and correlation of physical stability, dissolution behaviour and interaction parameter of amorphous solid dispersions of telmisartan: a drug development perspective. *Eur. J. Pharm. Sci.* **2013**, *49*, 723−731.
(43) Cook, M. T.; Tzortzis, G.; Charalampopoulos, D.; Khutoryanskiy, V. V. Microencapsulation of probiotics for gastro-intestinal delivery. *J. Controlled Release* **2012**, *162*, 56−67.
(44) Maheshwari, C.; André, V.; Reddy, S.; Roy, L.; Duarte, T.; Rodríguez-Hornedo, N. Tailoring aqueous solubility of a highly soluble compound via cocrystallization: effect of coformer ionization, pH max and solute−solvent interactions. *CrystEngComm* **2012**, *14*, 4801−4811.
(45) Serajuddin, A. T. Salt formation to improve drug solubility. *Adv. Drug Delivery Rev.* **2007**, *59*, 603−616.

DOI: 10.1021/acsomega.8b02144
ACS Omega 2018, 3, 15380−15388